Xenobiotic CAR activators induce Dlk1-Dio3 locus non-coding RNA expression in mouse liver

Pouché , Lucie; Vitobello, Antonio; Römer, Michael ; Glogovac, Milica ; MacLeod, A. Kenneth; Ellinger-Ziegelbauer, Heidrun

Published in:
Toxicological Sciences

DOI:
10.1093/toxsci/kfx104

Publication date:
2017

Document Version
Peer reviewed version

OXFORD UNIVERSITY PRESS | Toxicological Sciences

Xenobiotic CAR activators induce Dlk1-Dio3 locus non-coding RNA expression in mouse liver

Journal:	*Toxicological Sciences*
Manuscript ID	TOXSCI-16-0705.R1
Manuscript Type:	Research Article
Date Submitted by the Author:	n/a
Complete List of Authors:	Pouche, Lucie; Novartis Institutes for Biomedical Research, Preclinical Safety, Translational Medicine Vitobello, Antonio; Novartis Institutes for Biomedical Research, Preclinical Safety, Translational Medicine Römer, Michael; University of Tübingen, Department of Computer Science Glogovac, Milica; Novartis Pharma AG, Novartis Business Services MacLeod, A. Kenneth; University of Dundee, Division of Cancer Research, Jacqui Wood Cancer Centre Ellinger-Ziegelbauer, Heidrun; Bayer Pharma AG, Westphal, Magdalena; Novartis Institutes for Biomedical Research, Preclinical Safety, Translational Medicine Dubost, Valerie; Novartis Institutes for Biomedical Research, Preclinical Safety, Translational Medicine Stiehl, Daniel; Novartis Institutes for Biomedical Research, Preclinical Safety, Translational Medicine Dumotier, Bérengère; Novartis Institutes for Biomedical Research, Preclinical Safety, Translational Medicine Fekete, Alexander; Novartis Institutes for Biomedical Research Moulin, Pierre; Novartis Institutes for Biomedical Research, Preclinical Safety, Translational Medicine Zell, Andreas; University of Tübingen, Center for Bioinformatics Schwarz, Michael; University of Tuebingen, Toxicology; Moreno, Rita; University of Dundee, Division of Cancer Research, Jacqui Wood Cancer Centre Huang, Jeffrey T. J. ; University of Dundee, Biomarker and Drug Analysis Core Facility, School of Medicine Elcombe, Clifford; CXR Biosciences, ; Henderson, Colin; University of Dundee, Cancer Research UK, Molecular Pharmacology Unit Wolf, C. Roland; University of Dundee, Cancer Research UK, Medical Research Institute Moggs, Jonathan; Novartis Pharma AG, Safety Profiling & Assessment, Investigative Toxicology Terranova, Remi; Novartis Institutes for Biomedical Research, Preclinical Safety, Translational Medicine
Key Words:	Cancer Risk Assessment, Constitutive Androstane Receptor (CAR), biomarkers < Safety Evaluation, non-genotoxic < Carcinogenesis, Dlk1-

	Dio3 cluster long non-coding RNAs

Xenobiotic CAR activators induce Dlk1-Dio3 locus non-coding RNA expression in mouse liver

Lucie Pouché*, Antonio Vitobello*, Michael Römer[1], Milica Glogovac, A. Kenneth MacLeod, Heidrun Ellinger-Ziegelbauer[1], Magdalena Westphal, Valérie Dubost, Daniel Philipp Stiehl, Bérengère Dumotier, Alexander Fekete, Pierre Moulin, Andreas Zell[1], Michael Schwarz[1], Rita Moreno, Jeffrey T. J. Huang, Cliff R. Elcombe[1], Colin J. Henderson[1], C. Roland Wolf[1], Jonathan G. Moggs[1], Rémi Terranova**

Author affiliations:

Lucie Pouché: **contributed equally to this work*, Preclinical Safety, Translational Medicine, Novartis Institutes for Biomedical Research, CH-4057 Basel, Switzerland, pouche.lucie@gmail.com

Antonio Vitobello: **contributed equally to this work*, Preclinical Safety, Translational Medicine, Novartis Institutes for Biomedical Research, CH-4057 Basel, Switzerland, antonio.vitobello@novartis.com

Milica Glogovac: Novartis Business Services, Novartis Pharma, CH-4057 Basel, Switzerland, milica.glogovac@novartis.com

Michael Römer: Department of Computer Science, University of Tübingen, Sand 1, 72076 Tübingen, Germany, michael.roemer@uni-tuebingen.de

A. Kenneth MacLeod: Division of Cancer Research, Jacqui Wood Cancer Centre, University of Dundee, James Arrott Drive, Ninewells Hospital And Medical School, Dundee, DD1 9SY, United Kingdom, K.A.Z.MacLeod@dundee.ac.uk

Heidrun Ellinger-Ziegelbauer: Investigational Toxicology, GDD-GED-Toxicology, Bayer Pharma AG, 42096 Wuppertal, Germany, heidrun.ellinger-ziegelbauer@bayer.com

Magdalena Westphal: Preclinical Safety, Translational Medicine, Novartis Institutes for Biomedical Research, CH-4057 Basel, Switzerland, magdalena.westphal@novartis.com

Valérie Dubost: Preclinical Safety, Translational Medicine, Novartis Institutes for Biomedical Research, CH-4057 Basel, Switzerland, valerie.dubost@novartis.com

Daniel Philipp Stiehl: Preclinical Safety, Translational Medicine, Novartis Institutes for Biomedical Research, CH-4057 Basel, Switzerland, daniel.stiehl@novartis.com

Bérengère Dumotier: Preclinical Safety, Translational Medicine, Novartis Institutes for Biomedical Research, CH-4057 Basel, Switzerland, berengere.dumotier@novartis.com

Alexander Fekete: Preclinical Safety, Translational Medicine, Novartis Institutes for Biomedical Research, Inc. 250 Massachusetts Avenue, Cambridge, MA 02139, United States, alexander.fekete@novartis.com

Pierre Moulin: Preclinical Safety, Translational Medicine, Novartis Institutes for Biomedical Research, CH-4057 Basel, Switzerland, pierre.moulin@novartis.com

Andreas Zell: Department of Computer Science, University of Tübingen, Sand 1, 72076 Tübingen, Germany, andreas.zell@uni-tuebingen.de

Michael Schwarz: Department of Toxicology, University of Tübingen, Wilhelmstr. 56, 72074 Tübingen, Germany, michael.schwarz@uni-tuebingen.de

Rita Moreno: Division of Cancer Research, Jacqui Wood Cancer Centre, University of Dundee, James Arrott Drive, Ninewells Hospital And Medical School, Dundee, DD1 9SY, United Kingdom, ritadorta@gmail.com

Jeffrey T. J. Huang: Biomarker and Drug Analysis Core Facility, School of Medicine, University of Dundee, Jacqui Wood Cancer Centre, Ninewells Hospital, Dundee, DD1 9SY, United Kingdom, j.t.j.huang@dundee.ac.uk

Cliff R. Elcombe: CXR Biosciences Ltd., 2 James Lindsay Place, Dundee Technopole, Dundee Scotland DD1 5JJ, cliffelcombe@cxrbiosciences.com

Colin J. Henderson: Division of Cancer Research, Jacqui Wood Cancer Centre, University of Dundee, James Arrott Drive, Ninewells Hospital And Medical School, Dundee, DD1 9SYMedical Research Institute, University of Dundee, Dundee, United Kingdom, c.j.henderson@dundee.ac.uk

C. Roland Wolf: Division of Cancer Research, Jacqui Wood Cancer Centre, University of Dundee, James Arrott Drive, Ninewells Hospital And Medical School, Dundee, DD1 9SYMedical Research Institute, University of Dundee, Dundee, United Kingdom, c.r.wolf@dundee.ac.uk

Jonathan G. Moggs: Preclinical Safety, Translational Medicine, Novartis Institutes for Biomedical Research, CH-4057 Basel, Switzerland, jonathan.moggs@novartis.com

Rémi Terranova: **corresponding author, Preclinical Safety, Translational Medicine, Novartis Institutes for Biomedical Research, CH-4057 Basel, Switzerland, remi.terranova@novartis.com

[1]MARCAR consortium member

*Contributed equally to the work

**Corresponding author

Keywords: *Dlk1-Dio3* cluster, non-coding RNAs, Constitutive Androstane Receptor (CAR), Non-genotoxic Carcinogenesis (NGC), Cancer Risk Assessment, Phenobarbital, Chlordane

Abstract

Derisking xenobiotic-induced non-genotoxic carcinogenesis (NGC) represents a significant challenge during the safety assessment of chemicals and therapeutic drugs. The identification of robust mechanism-based NGC biomarkers has the potential to enhance cancer hazard identification. We previously demonstrated Constitutive Androstane Receptor (CAR) and WNT signaling-dependent up-regulation of the pluripotency associated *Dlk1-Dio3* imprinted gene cluster non-coding RNAs (ncRNAs) in the liver of mice treated with tumor-promoting doses of phenobarbital (PB). Here, we have compared phenotypic, transcriptional and proteomic data from wild-type, CAR/PXR double knock-out and CAR/PXR double humanized mice treated with either PB or chlordane, and show that hepatic *Dlk1-Dio3* locus long ncRNAs are upregulated in a CAR/PXR-dependent manner by two structurally distinct CAR activators. We further explored the specificity of *Dlk1-Dio3* locus ncRNAs as hepatic NGC biomarkers in mice treated with additional compounds working through distinct NGC modes of action. We propose that up-regulation of *Dlk1-Dio3* cluster ncRNAs can serve as an early biomarker for CAR activator-induced non-genotoxic hepatocarcinogenesis and thus may contribute to mechanism-based assessments of carcinogenicity risk for chemicals and novel therapeutics.

1. Introduction

Assessing the risk for xenobiotic-induced non-genotoxic carcinogenesis (NGC) is a major challenge for safety scientists. This is exemplified by the broad range of cancer hazard identification strategies that are selectively deployed during the preclinical development of novel therapeutics based on their modality, mode of action, disease indication, and phase of development (Moggs et al. 2016). Derisking drug-induced carcinogenicity would benefit from the development of reliable mechanism-based biomarkers that enable early cancer hazard identification and also enhance mechanistic insight for positive tumor findings in life-time rodent carcinogenicity studies.

The liver is a major target organ for xenobiotic-induced NGC. We have used Phenobarbital (PB), an anticonvulsant commonly used for treatment of epilepsy and other seizures, as a model compound to study mechanisms underlying liver NGC mechanisms. PB indirectly activates CAR through molecular pathways that have been reported to include the inhibition of epidermal growth factor receptor signaling (Mutoh et al. 2013). PB-mediated liver tumor promotion in mice is dependent on CAR and β-catenin (Huang et al. 2005; Rignall et al. 2011; Yamamoto et al. 2004). Furthermore, β-catenin harbours activating mutations in most CAR-dependent mouse liver tumors (Unterberger et al. 2014; Aydinlik et al. 2001). Through integrated molecular profiling, we previously uncovered an early, progressive and long-lasting, CAR- and β-catenin-dependent up-regulation of the *Dlk1-Dio3* imprinted cluster ncRNAs in perivenous hepatocytes of mice treated with tumor-promoting doses of PB (Lempiainen et al. 2013; Luisier et al. 2014). Several groups have reported a potential role for *Dlk1-Dio3* derived non-coding transcripts in stem cell pluripotency (Liu et al. 2010; Stadtfeld and Hochedlinger 2010). The overexpression of the human

Dlk1-Dio3 miRNA cluster was also positively correlated with expression of hepatocellular carcinoma (HCC) stem cells markers and was also associated with poor survival rate in HCC patients (Luk et al. 2011). Many of the *Dlk1-Dio3* cluster miRNAs are differentially expressed in hepatocellular carcinomas (Benetatos, Vartholomatos, and Hatzimichael 2014; Cui et al. 2015; Xu et al. 2013; Yin et al. 2013). Together, these observations highlight a pathophysiological role for *Dlk1-Dio3* ncRNA dysregulation in liver cancer and support their functional relevance as early NGC biomarkers.

Xenobiotic-induced activation of CAR and/or Pregnane X receptor (PXR) triggers an immediate activation of specific subsets of cytochrome P450 (CYP)-encoding genes, including the *Cyp2b* and *Cyp2c* family isoforms. CAR and PXR trans-activate a large battery of genes involved in phase I oxidation and phase II conjugation pathways that contribute to xenobiotic metabolism. PXR and CAR receptors have overlapping functions in the regulation of xenobiotic metabolism genes such as *Cyp3a*, whilst CAR- and PXR-specific target genes have also been identified (Cui and Klaassen 2016; Wei et al. 2002). Chronic CAR activation by PB or other (in)direct activators is associated with hepatocellular carcinoma, liver injury, glucose metabolism and cholesterol homeostasis (Kobayashi et al. 2015). It was previously proposed that monitoring of P450-encoding genes such as *Cyp2b10*, one of the most strongly regulated CAR targets, could provide a robust surrogate biomarker of CAR activation in drug-induced mouse liver tumors (Hoflack et al. 2012).

To explore further the NGC-specificity and CAR-activation dependence of xenobiotic-induced liver *Dlk1-Dio3* long non-coding RNAs *(lnc*RNAs*)* activation, we compared phenotypic, transcriptional and proteomic data from wild-type and CAR/PXR transgenic C57BL/6 mouse models following *in vivo* treatment with PB and the

pesticide-derived CAR-activator chlordane (Malarkey 1995; Moser and Smart 1989; Ruch et al. 1990). We further investigated selected transcriptional profiles from mouse liver samples exposed to additional NGC compounds that work through different modes of action (MoA), and show that up-regulation of hepatic *Dlk1-Dio3* cluster non-coding RNAs represents a common feature of CAR-activating compounds. Our study highlights *Dlk1-Dio3* imprinted cluster lncRNAs as potential CAR activator-specific hepatic biomarkers that warrant further evaluation as tools for mechanism-based safety assessment of xenobiotic-induced liver non-genotoxic carcinogenesis.

2. Material and methods

2.1. Ethics statement

In vivo mouse studies were performed either according to the Institutional Guidelines of the University of Tübingen (Rignall et al. 2011) or in conformity with the Swiss Animal Welfare Law -Animal Licenses No. 2345 by “Kantonales Veterinäramt Basel-Stadt” [Cantonal Veterinary Office, Basel] and No. 5041 by “Kantonales Veterinäramt Baselland” [Cantonal Veterinary Office, Basel Land].

2.2. Animal husbandry and dosing

For the chlordane *in vivo* study, eight to eleven week-old male CAR^{h}-PXR^{h}, CAR^{KO}-PXR^{KO} and wild-type C57BL/6 mice were used (Taconic, Germany). Animals were randomly allocated in groups of 5 per treatment and time point. Mice were checked daily for activity and behavior and administered with chlordane (Sigma-Aldrich [St Louis, MO] #PS75, 8 mg/kg/day), or corn oil (vehicle) by oral gavage – treatment doses were selected based on (Ross et al. 2010; Barrass et al. 1993). After 28 days (t=28) of treatment, the compound was withdrawn and the recovery group animals kept for a further 28 days for reversibility assessment (t=56). At sacrifice, on day 29 (2 hrs post-dose) and 57 (recovery period), blood was sampled for pharmacokinetics (PK) analysis and hepatic lobes were collected and either frozen in liquid nitrogen and stored at −80°C for subsequent analyses or fixed in neutral phosphate-buffered formalin and paraffin-embedded (FFPE). To ensure sample homogeneity for different molecular profiling methods, frozen liver samples were reduced to powder with Covaris Cryoprep system (Covaris Inc., Woburn, MA) and aliquoted on dry ice. For the Phenobarbital study comparison, samples from the *in vivo* study using C57BL/6

Wild-type (WT), CAR/PXR double knockout (CAR^{KO}-PXR^{KO}) and humanized CAR/PXR (CAR^{h}-PXR^{h}) mice chronically exposed for 28 days (t=28), 91 days (t=91) or 91 days followed by 28 days of recovery (t=119) from (Luisier et al. 2014) were analyzed. Additional justification on compounds dose selection is available in Supplementary Material and Methods.

2.3. Cross-compound data mining, Affymetrix labeling, GeneChip processing and gene expression analysis

We performed data mining of *in vivo* gene expression profiles produced by the MARCAR consortium (http://www.imi-marcar.eu/) encompassing six well-known liver NGC compounds: Phenobarbital (PB), Pirinixic acid (Wy), Piperonyl Butoxide (PBO), 1,4-dichlorobenzene (DCB), Cyproterone acetate (CPA), and methapyrilene (Mpy). Pioglitazone (Pio) was used as a non-hepatocarcinogen compound and CITCO as a human specific CAR activator. Data sets of Wy, PBO, DCB, CPA, MPY, PB, CITCO and Pio studies were publically released and available at NCBI's GEO (GSE68364 and GSE60684). Affymetrix labeling and GeneChip (Mouse Genome 430 2.0 Array) processing were conducted as described in (Lempiainen et al. 2013). Heatmaps were built using TIBCO Spotfire®. GeneChip and qPCR expression data analyses were described in Supplementary Materials and Methods.

2.4. RT-qPCR analyses

RNA isolation and quantitative RT-PCR analyses were performed as previously described (Lempiainen et al. 2013) and are detailed in Supplementary Materials and Methods. All expression analyses are based on qPCR, primer sequences are provided in (Lempiainen et al. 2013) and Supplementary Materials and Methods. Data were analyzed using GraphPad Prism 7.0. Statistical significance of treated

versus untreated (vehicle) qPCR signal differences (n=5/group) were tested using unpaired t-tests with Welch's correction for unequal variance.

2.5. Proteomic analysis

Sample preparation, data acquisition and analysis by targeted high resolution single ion monitoring (tHR/SIM) *in vivo* 'stable isotope labelling by amino acids in cell culture' (SILAC) using a pathway-enhanced internal standard was carried out as described previously (MacLeod et al. 2015) (Supplementary Material and Methods). For generation of the hierarchical clustering heatmaps, Xcalibur files were processed using MaxQuant, version 1.4.1.2, (Cox and Mann 2008) and the integrated Andromeda search engine with the Uniprot Mus musculus (taxID: 10090) reference proteome set (44,455 entries, downloaded 03.12.14). Cysteine carbamidomethylation was set as a fixed modification, with N-terminal acetylation and methionine oxidation as variable modifications. The protein false discovery rate was set to 1%, minimum peptide length was 7 and a maximum of 2 miscleavages was allowed. Data were processed in Perseus (version 1.5.1.6). For each control/xenobiotic comparison, only proteins with ≥3 valid values were retained. Data were analyzed using GraphPad Prism 7.0. Statistical significance of treated versus untreated (vehicle) signal differences were tested using multiple unpaired t-tests on log2 transformed data. The p-values were adjusted using Holm-Sidak method, with alpha = 0.05.

For proteomics heatmap generation, individual animal data were normalised to the mean of the control group, $\log_2$-transformed and missing values imputed from normal distribution. Clustering was generated in R using the RStudio interface with the gplots and RColorBrewer packages.

2.6. In situ hybridization (ISH) and Immunohistochemistry (IHC)

Meg3 in situ hybridization (ISH) and glutamine synthetase (GS) immunohistochemistry (IHC) were conducted on liver samples of chlordane- and PB-treated animals as previously described (Lempiainen et al. 2013), detailed in Supplementary Materials and Methods.

3. Results

3.1. Comparable liver phenotypic and histopathologic responses following 28 days *in vivo* PB and chlordane treatment of mice.

We previously showed that the *Dlk1-Dio3* transcriptional response mediated by PB is CAR-dependent (Lempiainen et al. 2013; Luisier et al. 2014). In order to further evaluate the specificity of this candidate NGC biomarker for CAR activators, we compared the effects of PB and chlordane in the liver of WT, CAR/PXR double knockout (CAR^{KO}-PXR^{KO}) and double humanized (CAR^{h}-PXR^{h}) C57BL/6 animals after 28 days (t=28) treatment with either compound (**Fig. 1A**). Akin to PB, chlordane is a NGC compound which induces hepatomegaly characterized by hypertrophy and hyperplasia and acts through robust CAR activation (Ross et al. 2010; Barrass et al. 1993; Malarkey 1995; Whysner et al. 1998).

No significant body weight differences were observed comparing 28 days PB and chlordane treated samples (**Table 1**). Microscopically, similar histopathological changes were observed in liver, characterized by moderate centrilobular hepatocellular hypertrophy in WT after 28 days with both treatments. Centrilobular hepatocytes showed cytoplasmic changes with an eosinophilic and/or granular basophilic cytoplasm in chlordane treated samples (data not shown). Comparable, moderate to marked, changes were also made in CAR^{h}-PXR^{h} animals. No morphological alterations were present in CAR^{KO}-PXR^{KO} mice with either compound. Following recovery, centrilobular hypertrophy and cytoplasmic changes were still present in both WT and CAR^{h}-PXR^{h} mice in chlordane- and PB-treated samples, although less pronounced in humanized groups.

Interestingly, plasma concentration of chlordane-treated samples showed appreciable compound levels after 28 days of recovery (t=56, 1 µg/mL in WT animals) consistent with chlordane's long half-life (Zucker 1985). PB on the other hand was undetectable after 28 days recovery (t=56) (**Table 1**). Overall, the liver histopathological changes induced by chlordane are CAR/PXR-activation dependent and similar to those induced by PB.

3.2. Both chlordane and PB induce *Dlk1-Dio3* lncRNA up-regulation in perivenous hepatocytes

We next investigated the transcriptional response of *Dlk1-Dio3* lncRNAs in chlordane and PB treated mice. Using RT-qPCR, we profiled the expression of both coding and long non-coding transcripts throughout the *Dlk1-Dio3* cluster in 28-day PB and chlordane liver study samples (t=28) (**Fig. 1A**). The imprinted *Dlk1-Dio3* locus contains three protein coding genes (*Dlk1, Dio3* and *Rtl1*) expressed from the paternally inherited allele, and several maternal-of-origin lncRNAs (*Meg3*, *anti-Rtl1*, *Rian* and *Mirg*) (Benetatos, Vartholomatos, and Hatzimichael 2014) (**Fig. 1B**). Strikingly, PB and chlordane triggered comparable transcriptional activation of *Meg3, anti-Rtl1*, *Rian* and *Mirg* lncRNAs in wild-type animals (**Fig. 1C**) with no detectable activation of the coding genes *Dlk1* and *Dio3*. Consistent with long half-life of chlordane (**Table 1**), increased levels of *Meg3, anti-Rtl1, Mirg* and *Cyp2b10* expression were observed in chlordane (but not PB) recovery group animals (t=56 and t=119 respectively) (**Supplementary Fig.S1**).

We had previously shown that *Meg3* expression occurs within a specific subset of perivenous hepatocytes expressing glutamine synthetase (GS) following PB treatment (Lempiainen et al. 2013). The *Glul* gene encoding for the GS protein is a

target regulated positively by the WNT signaling pathway and is also expressed in PB-promoted tumors (Loeppen et al. 2002). Immunohistochemistry (IHC) and *in situ* hybridization (ISH) directed against GS and *Meg3* respectively showed similar *Meg3* lncRNA distribution and no apparent change in GS expression levels with either compound in 28-day treated samples (**Fig. 1D**), altogether consistent with CAR- and β-catenin dependence of the *Dlk1-Dio3* lncRNAs activation.

3.3. Differential liver *Dlk1-Dio3* lncRNA activation in humanized CAR/PXR mice following PB versus chlordane exposure

CAR and PXR double knockouts (CAR^{KO}-PXR^{KO}) and double humanized CAR and PXR (CAR^{h}-PXR^{h}) mouse models were used to examine CAR/PXR dependencies and potential species differences in receptor-dependent responses to chlordane (**Fig. 1A**). As described previously (Luisier et al. 2014), PB led to comparable activation of *Dlk1-Dio3* lncRNAs in WT and humanized mice models (approx. 20 fold increase over vehicle controls - compare **Fig. 2A** and **Fig. 1C**, red bars). In contrast, while chlordane treatment led to over 10 fold induction of *Dlk1-Dio3* lncRNAs in WT animals (**Fig. 1C**, orange bars), the cluster was minimally induced (approx. 2.5 fold induction over control) upon chlordane treatment of CAR^{h}-PXR^{h} animals (**Fig. 2A**).Consistently, lower levels of *Cyp2b10* (**Fig. 2C**) were also detected in chlordane-treated CAR^{h}-PXR^{h} mice expressing hCAR (**Fig. 2D**) as compared to WT animals. KO animal models showed no *Meg3* expression (**Fig. 2B**) and no detectable *Cyp2b10* (**Fig. 2C**) activation upon chlordane treatment, consistent with the previously reported CAR dependence of PB effects (Luisier et al. 2014). The differential transcriptional responses observed for PB versus chlordane in humanized

CAR/PXR mice might be related to distinct, possibly species-specific, mechanisms of CAR activation by chlordane.

3.4. Proteome-based analyses of xenobiotic metabolism pathways in WT and CAR^h-PXR^h mouse liver following PB and chlordane exposure.

To further investigate the transcriptomic differences observed in CAR^h-PXR^h animals upon chlordane and PB treatments, we next performed peptide quantification using stable isotope labelling by amino acids in cell culture (SILAC) analysis of a wide range of enzymes implicated in xenobiotic metabolism using liver tissues from WT and humanized animals treated for 28 days with PB or chlordane. In WT animal samples, we found a comparable pattern of phase I cytochrome P450 protein expression following chlordane and PB treatments (**Fig. 3**). Cyp2b10, one of the strongest activated protein targets, showed significantly increased protein expression levels following both chlordane and PB treatment (**Fig. 3**). Selected proteins were strongly induced by PB but not by chlordane (e.g. Cyp2c54 and Cyp2c55), or inversely were more strongly induced by chlordane than PB (e,g. Por, Ces2a, Gstm3 and Gstt3), in WT animals (**Fig. 3, Supplementary Fig. S3 and S4**). Together these data suggest that the repertoire of xenobiotic genes activated by both compounds is largely but not fully overlapping. It is noteworthy that we also found consistent transcriptional and protein level induction in PB-treated WT mice (**Supplementary Fig. S2**). Consistent with the lower *Cyp2b10* transcriptional expression in CAR^h-PXR^h animals (**Fig 2C**), we observed reduced levels of a number of measured peptides corresponding to Cyp2b10/2b23, Cyp2c55 and Por enzymes in chlordane-treated humanized animals (**Fig.3, arrowed**). Additional Phase I and Phase II enzymes, such

as Ces2a and Gstt3 also displayed differential activation by chlordane in the CAR^{h}-PXR^{h} transgenic model (**Supplementary Fig. S3 and S4, arrowed**), suggesting that the humanized CAR model does not conserve the ability to regulate the entire mouse repertoire of xenobiotic metabolizing enzymes upon chlordane exposure. Together, these results highlight potential differences in chlordane and PB modes of action.

3.5. CAR activator specificity of *Dlk1-Dio3* lncRNA upregulation in mouse liver

We next evaluated microarray-based liver transcriptomic profiles derived from mice treated with a panel of structurally distinct rodent non-genotoxic carcinogens that work through distinct modes of action (studies were conducted Innovative Medicines Initiative MARCAR consortium http://www.imi-marcar.eu/; original gene expression profiling data available in Gene Expression Omnibus (GEO) under GSE68364 and GSE60684). For enhanced comparability, among all studies available, we selected data based on (i) study duration, selecting for studies of 28 days and above duration, at a stage when *Dlk1-Dio3* lncRNAs have been detected unambiguously upon PB treatment in B6C3F1 or C57BL/6 mice (Lempiainen et al. 2013; Luisier et al. 2014) and (ii) study strain, C57BL/6 studies were chosen to limit the inter-strain variability of the response. All available compound studies fulfilling these conditions were selected and included one cross-species CAR activator (PB), one human-specific CAR activator (CITCO) and five rodent liver NGCs acting through alternative or unidentified MoAs (pirinixic acid (WY), piperonyl butoxide (PBO), 1,4-dichloro-benzene (DCB), cyproterone acetate (CPA) and methapyrilene (MPA)). Pioglitazone (Pio), a bladder NGC in male rats, was included as a negative control compound for mouse hepatic NGC (detailed in **Supplementary Table S1**).

To compare the CAR activator-dependent effects on xenobiotic metabolism, we selected a subset of candidate CAR-dependent target genes involved in phase I and II xenobiotic metabolism (based on published CAR^{KO}, CAR^{KO}-PXR^{KO} animal models or on experiments conducted on PB treated hepatocytes - detailed in **Supplementary Table S2** and references within). While we detected the expected CAR-dependent activation of the selected xenobiotic response genes upon PB treatment, we also observed activation of *Cyb2b10* and other selected xenobiotic metabolism genes upon treatment with a range of distinct hepatic NGCs (**Fig. 4**). Specifically, *Cyp2b10* expression was strongly regulated by CPA and DCB, and also by Pioglitazone (Pio), a PPARγ agonist that we included as a negative control for liver NGC (Log_2FC from 6.99 to 7.67 for the three compounds, $p<0.001$, **Supplementary Table S3**). These data indicate that multiple signaling pathways can converge to mediate *Cyp* gene regulation. The CAR dependency of induction of *Cyp2b* and *Cyp2c* gene expression upon PB treatment was confirmed in CAR^{KO}-PXR^{KO} mice, as previously reported (Kobayashi et al. 2015).

Among the six rodent hepatic NGCs tested in this experiment, only PB treated liver samples showed increased *Meg3* and *Rian* expression (*Meg3* Log_2FC close to 2 in wild-type and humanized models upon 28 and 91 days of PB treatment, absent in CAR^{KO}-PXR^{KO} animals) (**Fig. 4**). None of the other five hepatic NGCs led to a significant induction of Meg3 or Rian regardless of the mouse strains or durations of exposure that were tested. CITCO, a direct and human-specific CAR agonist (Yang and Wang 2014), minimally increased the expression of Phase I and Phase II genes in CAR^{h}-PXR^{h} samples (Log_2FC= 5.94 and 2.72 in CAR^{h}-PXR^{h} mice, versus 0.69 and 0.28 in WT for *Cyp2b10* and *Cyp2c55* respectively), confirming the human specificity of CITCO-mediated CAR activation (**Fig. 4)** (Maglich et al. 2003).

However, we did not observe significant transcriptional activation of *Meg3* and *Rian* expression levels in humanized CAR/PXR mice under these experimental conditions. Taken together, these results suggest that the up-regulaton of *Dlk1-Dio3* lncRNA expression represents an early biomarker for CAR activator-induced mouse liver tumor promotion.

4. Discussion

Non-Genotoxic Carcinogenesis is a key safety assessment consideration for the development of chemicals and therapeutic drugs. There are currently no suitable short-term assays for predicting NGC. The identification of mechanism-based NGC biomarkers would provide industry and regulatory scientists with new tools and opportunities for earlier decision-making, mitigation of positive carcinogenicity findings and enhanced cancer risk assessment. There are, however, a number of significant challenges associated with the identification and application of NGC biomarkers (Moggs et al. 2016). Firstly, multiple combinations and chronologies of cancer hallmarks contribute to tumorigenicity and thus the detection of individual drug-induced neoplastic risk molecular indicators is not likely to be optimal for predicting diverse mechanisms of xenobiotic-induced carcinogenesis. Secondly, the identification of predictive transcriptomic NGC biomarkers in rodent carcinogenicity studies is confounded by the heterogeneity of drug-induced rodent tumors that cover a broad range of tissue-, gender-, strain- and species-specific mechanisms. Furthermore, the potential contributions from on- or off-target properties of NGC compounds makes the determination of mode of action and assessment of human relevance very challenging.

Nevertheless, mechanistic studies that integrate phenotypically-anchored molecular and biochemical biomarkers can be used to support the interpretation of drug-induced tumors and in some cases provide valuable perspectives on potential relevance in humans. Although numerous publications report extensive efforts to identify predictive transcriptomic biomarkers for NGC, this has proved challenging even for a single target organ such as the liver (Kossler et al. 2015; Ellinger-Ziegelbauer et al. 2011; Fielden et al. 2011). We propose that the validation of such

molecular biomarkers will be greatly enhanced by establishing functional relationships to known cancer hallmarks. This is exemplified by the identification of *Dlk1-Dio3* imprinted gene cluster non-coding RNAs as novel candidate biomarkers for phenobarbital-induced liver tumor promotion (Lempiainen et al. 2013). The induction of *Dlk1-Dio3* non-coding RNAs by phenobarbital is dependent on both constitutive androstane receptor (CAR) and β-catenin signalling pathways, consistent with a CAR activator-mediated hepatocarcinogenesis mode of action. Importantly, *Dlk1-Dio3* non-coding RNAs have recently been associated with stem cell pluripotency in mice and various neoplasms in humans. In addition, the perivenous localization of phenobarbital-induced *Dlk1-Dio3* non-coding RNAs occurs in a region of the liver that was recently associated with Wnt signalling-dependent stem cell-like properties (Wang et al. 2015; Planas-Paz et al. 2016). Together, these functional relationships imply that sub-population of hepatocytes may be prone to drug-induced reprogramming and de-differentiation and that biomarkers such as *Dlk1-Dio3* non-coding RNAs might serve as useful early molecular indicators for CAR-mediated hepatocarcinogenesis (**Supplementary Figure S5**).

Specifically, in this paper, we have compared phenotypic, histopathological, transcriptional and proteomic responses following treatment with the cross-species CAR activators, PB and chlordane, and further compared key transcriptional signatures with seven other NGC compounds working through a range of MoAs (**Supplementary Table S1**), including the human-specific direct CAR activator CITCO. We find that the xenobiotic metabolism gene *Cyp2b10* is upregulated by several distinct hepatic NGCs as well as the PPARγ agonist Pioglitazone (a control comparator compound that is not associated with hepatic NGC). Although *Cyp2b10* induction in drug-induced mouse liver tumors has previously been proposed as a

surrogate biomarker of CAR activation (Hoflack et al. 2012), our data suggest that Cyp2b10 induction alone may lack the required specificity for an early mechanism-based biomarker of CAR-mediated NGC consistent with previous observations that induction of CYP2B1/2 liver enzymes failed to correlate with rodent NGC (Elcombe et al. 2002). In contrast, our data provide additional support to the CAR activator specificity of previously identified *Dlk1-Dio3* lncRNA candidate biomarkers for mouse liver tumor promotion (Lempiainen et al. 2013).

Since we used double transgenic (CAR^{KO}-PXR^{KO} and CAR^{h}-PXR^{h}) animals in the PB and chlordane *in vivo* studies, we cannot formally exclude the role of PXR activation and function in the identified molecular signature. CAR shares several common features with PXR, and they overlap at a number of target genes and xenobiotic activators (Yang and Wang 2014). Although previous studies in CAR and PXR KO models also identified differentially regulated xenobiotic targets (Maglich et al. 2002; Wei et al. 2002; Cui and Klaassen 2016), the strict specificity to CAR versus PXR may require further investigations.

While both cross-species CAR activators, PB and chlordane, led to *Dlk1-Dio3* lncRNA activation, consistent with its direct human CAR activation MoA (Maglich et al. 2003), CITCO did not lead to either xenobiotic genes or *Dlk1-Dio3* cluster lncRNA activation in WT animals (**Fig. 4**) and led to moderate *Cyp2b10* activation, without effect on *Dlk1-Dio3* lncRNAs in CAR/PXR humanized animals. The absence of lncRNA activation by CITCO is reminiscent of the significantly decreased lncRNA activation upon chlordane exposure in humanized animals and could be related to species-specific interactions upstream or downstream of CAR/PXR activation that could be perturbed in the human transgenic model (**Fig. 5**). In addition, CITCO acts through direct CAR binding and activation, and a conformational change of the hCAR

isoforms in transgenic animals might also explain the apparent differences in Cyp induction and lack of *Dlk1-Dio3* cluster activation. Alternatively, the exposure or duration of the study in the transgenic animal studies may not be sufficient to detect *Dlk1-Dio3* lncRNA activation. Finally, we note that only two long non-coding RNAs (*Meg3* and *Rian*) are represented on the microarray used to profile compounds in **Fig. 4** and thus we cannot exclude that CITCO induces alternate *Dlk1-Dio3* ncRNAs. Further analyses of the complete *Dlk1-Dio3* cluster transcriptional landscape following longer-term CITCO treatment in PXR^h-CAR^h animals would be necessary to extend these observations as well as to explore the relevance of this compound in liver carcinogenesis. Three of the compounds tested (CPA, DCB and Pio), in addition to PB and CITCO, led to significant activation of *Cyp2b10* and *Cyp2c55*. However, under the experimental conditions tested, they did not induce detectable microarray-based dysregulation of *Dlk1-Dio3* cluster lncRNAs *Meg3* or *Rian*. Interestingly, using CYP2B6LacZ reporter and CAR/PXR humanized mouse models, both DCB and CPA were recently characterized as CAR activators with DCB displaying a higher potency towards human CAR than mouse CAR, and CPA activating both CAR and PXR (CJH, CRW, unpublished, manuscript in preparation). While no microarray-based upregulation of the *Dlk1-Dio*3 lncRNAs *Meg3* and *Rian* was detected for either DCB or CPA, quantitative PCR-based expression data indicated upregulation of several non-coding miRNAs within the *Dlk1-Dio3* cluster for both of these compounds (unpublished MARCAR data), consistent with our proposal that CAR-activation leads to *Dlk1-Dio3* cluster ncRNA perturbations in liver NGC models. It is noteworthy that the *Dlk1-Dio3* cluster encodes one of the largest microRNA clusters in the mammalian genome, as well as numerous small nucleolar RNAs (snoRNAs). We previously demonstrated PB-mediated induction both lncRNAs and miRNAs from the *Dlk1-Dio3* locus (Lempiainen et al. 2013). Interestingly, some *Dlk1-Dio3* cluster

miRNAs appear to be transcribed as single polycistronic unit (Fiore et al. 2009) and many of these miRNAs have been reported to be differentially expressed in pathologic processes including various cancers (reviewed in (Benetatos et al. 2013)). In this manuscript we have evaluated the hepatic responsiveness of four *Dlk1-Dio3* cluster long-non-coding RNAs (Meg3, anti-Rtl1, Rian, Mirg) by qPCR (PB and chlordane), and of two *Dlk1-Dio3* cluster long-non-coding RNA (Meg3 and Rian) by microarray-based transcript profiling (panel of compounds in **Fig. 4**). We cannot exclude that the compounds tested induce further broad or specific changes of the *Dlk1-Dio3* non-coding RNAs landscape and thus further RNA-sequencing based assessments of *Dlk1-Dio3* ncRNA candidate biomarkers is warranted. Beyond their association with pluripotency (Liu et al. 2010; Stadtfeld and Hochedlinger 2010), the interest in investigating the expression profile on the *Dlk1-Dio3* cluster lncRNAs, has been reinforced by the discovery that they are able to form complexes with the epigenetic machinery, including Polycomb group proteins (Kaneko et al. 2014) and might be targeted to specific genes through the formation of RNA-DNA triplex structures (Mondal et al. 2015). These regulatory interactions (illustrated **Supplementary Figure S5**) could play an important role in cellular transformation.

5. Conclusions

In the present study we have demonstrated that a second CAR activator and mouse liver non-genotoxic carcinogen (i.e. chlordane) robustly induces perivenous *Dlk1-Dio3* non-coding RNA expression and we provide preliminary evidence that this candidate biomarker signature may indeed be specific for CAR-mediated hepatocarcinogenesis. Through comparing the response to chlordane and PB exposure in WT and humanized animals, we also point to the existence of undetermined co-effector phenomenon, upstream or downstream to CAR activation (**Fig. 5**). Since significant molecular, cellular and pathophysiologic differences exist between mammalian species and strains, further evaluation of *Dlk1-Dio3* cluster non-coding RNA functions, biomarker detection sensitivity, MoA specificity and human relevance, is warranted prior to use as an early indicator for CAR-mediated hepatocarcinogenesis. In particular, mapping species differences in the hepatic chromatin architecture of candidate non-genotoxic carcinogen effector genes such as *Dlk1-Dio3* ncRNAs may help predict the potential for NGC-mediated modulation in humans (AV, RT and JM, unpublished data).

Acknowledgements, Funding and conflicts of interest

Innovative Medicine Initiative Joint Undertaking (IMI JU) (115001) (MARCAR project; http://www.imi-marcar.eu/). This work was also supported by Cancer Research UK program grant C4639/A10822 awarded to C.R.W. All IMI-MARCAR consortium partners had a role in study design, data collection and analysis, decision to publish, or preparation of the manuscript. We would like to thank Sarah Brasa, Harri Lempiäinen for experimental and *in vivo* study support and Serge Winter and Wei Wu for the pharmacokinetics analyses of chlordane and Phenobarbital studies. We would like also to thank Chi-Hse Teng for the statistical analysis support. M.G., M.W., V.D., D.P.S., B.D., P.M., J.G.M. and R.T. are full time employees of Novartis Pharma. A.V. is a recipient of a Novartis Institutes for Biomedical Research Postdoctoral Fellowships. H.E.Z. is a full time employee of Bayer. C.R.E. is a full time employee of CXR Biosciences.

References

Aydinlik, H., T. D. Nguyen, O. Moennikes, A. Buchmann, and M. Schwarz. 2001. 'Selective pressure during tumor promotion by phenobarbital leads to clonal outgrowth of beta-catenin-mutated mouse liver tumors', *Oncogene*, 20: 7812-6.

Barrass, N., M. Stewart, S. Warburton, J. Aitchison, D. Jackson, P. Wadsworth, A. Marsden, and T. Orton. 1993. 'Cell proliferation in the liver and thyroid of C57Bl/10J mice after dietary administration of chlordane', *Environ Health Perspect*, 101 Suppl 5: 219-23.

Benetatos, L., E. Hatzimichael, E. Londin, G. Vartholomatos, P. Loher, I. Rigoutsos, and E. Briasoulis. 2013. 'The microRNAs within the DLK1-DIO3 genomic region: involvement in disease pathogenesis', *Cell Mol Life Sci*, 70: 795-814.

Benetatos, L., G. Vartholomatos, and E. Hatzimichael. 2014. 'DLK1-DIO3 imprinted cluster in induced pluripotency: landscape in the mist', *Cell Mol Life Sci*, 71: 4421-30.

Braeuning, A., R. Sanna, J. Huelsken, and M. Schwarz. 2009. 'Inducibility of drug-metabolizing enzymes by xenobiotics in mice with liver-specific knockout of Ctnnb1', *Drug Metab Dispos*, 37: 1138-45.

Cox, J., and M. Mann. 2008. 'MaxQuant enables high peptide identification rates, individualized p.p.b.-range mass accuracies and proteome-wide protein quantification', *Nat Biotechnol*, 26: 1367-72.

Cui, J. Y., and C. D. Klaassen. 2016. 'RNA-Seq reveals common and unique PXR- and CAR-target gene signatures in the mouse liver transcriptome', *Biochim Biophys Acta*.

Cui, W., Z. Huang, H. He, N. Gu, G. Qin, J. Lv, T. Zheng, K. Sugimoto, and Q. Wu. 2015. 'MiR-1188 at the imprinted Dlk1-Dio3 domain acts as a tumor suppressor in hepatoma cells', *Mol Biol Cell*, 26: 1416-27.

Elcombe, C. R., J. Odum, J. R. Foster, S. Stone, S. Hasmall, A. R. Soames, I. Kimber, and J. Ashby. 2002. 'Prediction of rodent nongenotoxic carcinogenesis: evaluation of biochemical and tissue changes in rodents following exposure to nine nongenotoxic NTP carcinogens', *Environ Health Perspect*, 110: 363-75.

Ellinger-Ziegelbauer, H., M. Adler, A. Amberg, A. Brandenburg, J. J. Callanan, S. Connor, M. Fountoulakis, H. Gmuender, A. Gruhler, P. Hewitt, M. Hodson, K. A. Matheis, D. McCarthy, M. Raschke, B. Riefke, C. S. Schmitt, M. Sieber, A. Sposny, L. Suter, B. Sweatman, and A. Mally. 2011. 'The enhanced value of combining conventional and "omics" analyses in early assessment of drug-induced hepatobiliary injury', *Toxicol Appl Pharmacol*, 252: 97-111.

Fielden, M. R., A. Adai, R. T. Dunn, 2nd, A. Olaharski, G. Searfoss, J. Sina, J. Aubrecht, E. Boitier, P. Nioi, S. Auerbach, D. Jacobson-Kram, N. Raghavan, Y. Yang, A. Kincaid, J. Sherlock, S. J. Chen, B. Car, and Carcinogenicity Working Group Predictive Safety Testing Consortium. 2011. 'Development and evaluation of a genomic signature for the prediction and mechanistic assessment of nongenotoxic hepatocarcinogens in the rat', *Toxicol Sci*, 124: 54-74.

Fiore, R., S. Khudayberdiev, M. Christensen, G. Siegel, S. W. Flavell, T. K. Kim, M. E. Greenberg, and G. Schratt. 2009. 'Mef2-mediated transcription of the

miR379-410 cluster regulates activity-dependent dendritogenesis by fine-tuning Pumilio2 protein levels', *EMBO J*, 28: 697-710.

Hoflack, J. C., L. Mueller, S. Fowler, A. Braendli-Baiocco, N. Flint, O. Kuhlmann, T. Singer, and A. Roth. 2012. 'Monitoring Cyp2b10 mRNA expression at cessation of 2-year carcinogenesis bioassay in mouse liver provides evidence for a carcinogenic mechanism devoid of human relevance: the dalcetrapib experience', *Toxicol Appl Pharmacol*, 259: 355-65.

Huang, W., J. Zhang, M. Washington, J. Liu, J. M. Parant, G. Lozano, and D. D. Moore. 2005. 'Xenobiotic stress induces hepatomegaly and liver tumors via the nuclear receptor constitutive androstane receptor', *Mol Endocrinol*, 19: 1646-53.

Kaneko, S., R. Bonasio, R. Saldana-Meyer, T. Yoshida, J. Son, K. Nishino, A. Umezawa, and D. Reinberg. 2014. 'Interactions between JARID2 and noncoding RNAs regulate PRC2 recruitment to chromatin', *Mol Cell*, 53: 290-300.

Klipper-Aurbach, Y., M. Wasserman, N. Braunspiegel-Weintrob, D. Borstein, S. Peleg, S. Assa, M. Karp, Y. Benjamini, Y. Hochberg, and Z. Laron. 1995. 'Mathematical formulae for the prediction of the residual beta cell function during the first two years of disease in children and adolescents with insulin-dependent diabetes mellitus', *Med Hypotheses*, 45: 486-90.

Kobayashi, K., M. Hashimoto, P. Honkakoski, and M. Negishi. 2015. 'Regulation of gene expression by CAR: an update', *Arch Toxicol*, 89: 1045-55.

Kossler, N., K. A. Matheis, N. Ostenfeldt, D. Bach Toft, S. Dhalluin, U. Deschl, and A. Kalkuhl. 2015. 'Identification of specific mRNA signatures as fingerprints for carcinogenesis in mice induced by genotoxic and nongenotoxic hepatocarcinogens', *Toxicol Sci*, 143: 277-95.

Lempiainen, H., P. Couttet, F. Bolognani, A. Muller, V. Dubost, R. Luisier, A. Del Rio Espinola, V. Vitry, E. B. Unterberger, J. P. Thomson, F. Treindl, U. Metzger, C. Wrzodek, F. Hahne, T. Zollinger, S. Brasa, M. Kalteis, M. Marcellin, F. Giudicelli, A. Braeuning, L. Morawiec, N. Zamurovic, U. Langle, N. Scheer, D. Schubeler, J. Goodman, S. D. Chibout, J. Marlowe, D. Theil, D. J. Heard, O. Grenet, A. Zell, M. F. Templin, R. R. Meehan, R. C. Wolf, C. R. Elcombe, M. Schwarz, P. Moulin, R. Terranova, and J. G. Moggs. 2013. 'Identification of Dlk1-Dio3 imprinted gene cluster noncoding RNAs as novel candidate biomarkers for liver tumor promotion', *Toxicol Sci*, 131: 375-86.

Liu, L., G. Z. Luo, W. Yang, X. Zhao, Q. Zheng, Z. Lv, W. Li, H. J. Wu, L. Wang, X. J. Wang, and Q. Zhou. 2010. 'Activation of the imprinted Dlk1-Dio3 region correlates with pluripotency levels of mouse stem cells', *J Biol Chem*, 285: 19483-90.

Loeppen, S., D. Schneider, F. Gaunitz, R. Gebhardt, R. Kurek, A. Buchmann, and M. Schwarz. 2002. 'Overexpression of glutamine synthetase is associated with beta-catenin-mutations in mouse liver tumors during promotion of hepatocarcinogenesis by phenobarbital', *Cancer Res*, 62: 5685-8.

Luisier, R., H. Lempiainen, N. Scherbichler, A. Braeuning, M. Geissler, V. Dubost, A. Muller, N. Scheer, S. D. Chibout, H. Hara, F. Picard, D. Theil, P. Couttet, A. Vitobello, O. Grenet, B. Grasl-Kraupp, H. Ellinger-Ziegelbauer, J. P. Thomson, R. R. Meehan, C. R. Elcombe, C. J. Henderson, C. R. Wolf, M. Schwarz, P. Moulin, R. Terranova, and J. G. Moggs. 2014. 'Phenobarbital induces cell cycle transcriptional responses in mouse liver humanized for constitutive androstane and pregnane x receptors', *Toxicol Sci*, 139: 501-11.

Luk, J. M., J. Burchard, C. Zhang, A. M. Liu, K. F. Wong, F. H. Shek, N. P. Lee, S. T. Fan, R. T. Poon, I. Ivanovska, U. Philippar, M. A. Cleary, C. A. Buser, P. M. Shaw, C. N. Lee, D. G. Tenen, H. Dai, and M. Mao. 2011. 'DLK1-DIO3 genomic imprinted microRNA cluster at 14q32.2 defines a stemlike subtype of hepatocellular carcinoma associated with poor survival', *J Biol Chem*, 286: 30706-13.

MacLeod, A. K., P. G. Fallon, S. Sharp, C. J. Henderson, C. R. Wolf, and J. T. Huang. 2015. 'An enhanced in vivo stable isotope labeling by amino acids in cell culture (SILAC) model for quantification of drug metabolism enzymes', *Mol Cell Proteomics*, 14: 750-60.

Maglich, J. M., D. J. Parks, L. B. Moore, J. L. Collins, B. Goodwin, A. N. Billin, C. A. Stoltz, S. A. Kliewer, M. H. Lambert, T. M. Willson, and J. T. Moore. 2003. 'Identification of a novel human constitutive androstane receptor (CAR) agonist and its use in the identification of CAR target genes', *J Biol Chem*, 278: 17277-83.

Maglich, J. M., C. M. Stoltz, B. Goodwin, D. Hawkins-Brown, J. T. Moore, and S. A. Kliewer. 2002. 'Nuclear pregnane x receptor and constitutive androstane receptor regulate overlapping but distinct sets of genes involved in xenobiotic detoxification', *Mol Pharmacol*, 62: 638-46.

Malarkey, David E. 1995. '<Carcinogenesis-1995-Malarkey-Chlordane.pdf>', *Carcinogenesis*, 16: 2617-25.

Moggs, Jonathan G., Timothy MacLachlan, Hans-Joerg Martus, and Philip Bentley. 2016. 'Derisking Drug-Induced Carcinogenicity for Novel Therapeutics', *Trends in Cancer*, 2: 398-408.

Mondal, T., S. Subhash, R. Vaid, S. Enroth, S. Uday, B. Reinius, S. Mitra, A. Mohammed, A. R. James, E. Hoberg, A. Moustakas, U. Gyllensten, S. J. Jones, C. M. Gustafsson, A. H. Sims, F. Westerlund, E. Gorab, and C. Kanduri. 2015. 'MEG3 long noncoding RNA regulates the TGF-beta pathway genes through formation of RNA-DNA triplex structures', *Nat Commun*, 6: 7743.

Moser, G. J., and R. C. Smart. 1989. 'Hepatic tumor-promoting chlorinated hydrocarbons stimulate protein kinase C activity', *Carcinogenesis*, 10: 851-6.

Mutoh, S., M. Sobhany, R. Moore, L. Perera, L. Pedersen, T. Sueyoshi, and M. Negishi. 2013. 'Phenobarbital indirectly activates the constitutive active androstane receptor (CAR) by inhibition of epidermal growth factor receptor signaling', *Sci Signal*, 6: ra31.

Omura, K., T. Uehara, Y. Morikawa, H. Hayashi, K. Mitsumori, K. Minami, M. Kanki, H. Yamada, A. Ono, and T. Urushidani. 2014. 'Detection of initiating potential of non-genotoxic carcinogens in a two-stage hepatocarcinogenesis study in rats', *J Toxicol Sci*, 39: 785-94.

Planas-Paz, L., V. Orsini, L. Boulter, D. Calabrese, M. Pikiolek, F. Nigsch, Y. Xie, G. Roma, A. Donovan, P. Marti, N. Beckmann, M. T. Dill, W. Carbone, S. Bergling, A. Isken, M. Mueller, B. Kinzel, Y. Yang, X. Mao, T. B. Nicholson, R. Zamponi, P. Capodieci, R. Valdez, D. Rivera, A. Loew, C. Ukomadu, L. M. Terracciano, T. Bouwmeester, F. Cong, M. H. Heim, S. J. Forbes, H. Ruffner, and J. S. Tchorz. 2016. 'The RSPO-LGR4/5-ZNRF3/RNF43 module controls liver zonation and size', *Nat Cell Biol*, 18: 467-79.

Rignall, B., A. Braeuning, A. Buchmann, and M. Schwarz. 2011. 'Tumor formation in liver of conditional beta-catenin-deficient mice exposed to a diethylnitrosamine/phenobarbital tumor promotion regimen', *Carcinogenesis*, 32: 52-7.

Ross, J., S. M. Plummer, A. Rode, N. Scheer, C. C. Bower, O. Vogel, C. J. Henderson, C. R. Wolf, and C. R. Elcombe. 2010. 'Human constitutive androstane receptor (CAR) and pregnane X receptor (PXR) support the hypertrophic but not the hyperplastic response to the murine nongenotoxic hepatocarcinogens phenobarbital and chlordane in vivo', *Toxicol Sci*, 116: 452-66.

Ruch, R. J., R. Fransson, S. Flodstrom, L. Warngard, and J. E. Klaunig. 1990. 'Inhibition of hepatocyte gap junctional intercellular communication by endosulfan, chlordane and heptachlor', *Carcinogenesis*, 11: 1097-101.

Smyth, G. K., J. Michaud, and H. S. Scott. 2005. 'Use of within-array replicate spots for assessing differential expression in microarray experiments', *Bioinformatics*, 21: 2067-75.

Stadtfeld, M., and K. Hochedlinger. 2010. 'Induced pluripotency: history, mechanisms, and applications', *Genes Dev*, 24: 2239-63.

Unterberger, E. B., J. Eichner, C. Wrzodek, H. Lempiainen, R. Luisier, R. Terranova, U. Metzger, S. Plummer, T. Knorpp, A. Braeuning, J. Moggs, M. F. Templin, V. Honndorf, M. Piotto, A. Zell, and M. Schwarz. 2014. 'Ha-ras and beta-catenin oncoproteins orchestrate metabolic programs in mouse liver tumors', *Int J Cancer*, 135: 1574-85.

Wang, B., L. Zhao, M. Fish, C. Y. Logan, and R. Nusse. 2015. 'Self-renewing diploid Axin2(+) cells fuel homeostatic renewal of the liver', *Nature*, 524: 180-5.

Wei, P., J. Zhang, D. H. Dowhan, Y. Han, and D. D. Moore. 2002. 'Specific and overlapping functions of the nuclear hormone receptors CAR and PXR in xenobiotic response', *Pharmacogenomics J*, 2: 117-26.

Whysner, J., F. Montandon, R. M. McClain, J. Downing, L. K. Verna, R. E. Steward, 3rd, and G. M. Williams. 1998. 'Absence of DNA adduct formation by phenobarbital, polychlorinated biphenyls, and chlordane in mouse liver using the 32P-postlabeling assay', *Toxicol Appl Pharmacol*, 148: 14-23.

Xu, W. P., M. Yi, Q. Q. Li, W. P. Zhou, W. M. Cong, Y. Yang, B. F. Ning, C. Yin, Z. W. Huang, J. Wang, H. Qian, C. F. Jiang, Y. X. Chen, C. Y. Xia, H. Y. Wang, X. Zhang, and W. F. Xie. 2013. 'Perturbation of MicroRNA-370/Lin-28 homolog A/nuclear factor kappa B regulatory circuit contributes to the development of hepatocellular carcinoma', *Hepatology*, 58: 1977-91.

Yamamoto, Y., R. Moore, T. L. Goldsworthy, M. Negishi, and R. R. Maronpot. 2004. 'The orphan nuclear receptor constitutive active/androstane receptor is essential for liver tumor promotion by phenobarbital in mice', *Cancer Res*, 64: 7197-200.

Yang, H., and H. Wang. 2014. 'Signaling control of the constitutive androstane receptor (CAR)', *Protein Cell*, 5: 113-23.

Yin, C., P. Q. Wang, W. P. Xu, Y. Yang, Q. Zhang, B. F. Ning, P. P. Zhang, W. P. Zhou, W. F. Xie, W. S. Chen, and X. Zhang. 2013. 'Hepatocyte nuclear factor-4alpha reverses malignancy of hepatocellular carcinoma through regulating miR-134 in the DLK1-DIO3 region', *Hepatology*, 58: 1964-76.

Zucker, E. . 1985. "Hazard Evaluation Division Standard Evaluation Procedure: Acute Toxicity Test for

Freshwater Fish." In, edited by National Technical U.S. Environmental Protection Agency and VA Information Service: Springfield.

Figure Legends

Figure 1. *Dlk1-Dio3* cluster response upon 28 days phenobarbital or chlordane exposure. (A) Experimental design of the chlordane and PB studies for molecular and phenotypic profiling (B) Architecture of *Dlk1-Dio3* genomic region illustrating parent-of-origin transcripts and differentially methylated regions (DMR) – methylated regions are represented with solid circles. (C) RT-qPCR analysis of *Dlk1-Dio3* genes (*Dlk1* and *Dio3*) and long non-coding RNAs (*Meg3, anti-Rtl1, Rian, Mirg*) expression in wild type (WT) mouse livers treated for 28 days with PB, chlordane or the relevant vehicle controls. Expression levels are indicated as mean ± SEM (n=5 biological replicates/group). Data were analyzed using GraphPad Prism 7.0. Statistical significance of treated versus untreated (vehicle) qPCR signal differences were tested using unpaired t-tests with Welch's correction for unequal variance, *p<0.05, **p<0.01. (D) *Meg3 in situ* hybridization and GS immunohistochemistry in 28 days PB or in chlordane treated livers with indicated vehicle controls. Water (H_2O), Corn Oil (CO).

Figure 2. *Dlk1-Dio3* cluster lncRNAs are differentially induced by PB and chlordane in humanized CAR/PXR animals. (A) *Dlk1-Dio3* coding and non-coding RNAs expression analysis in CAR^h-PXR^h mice after 28 days chlordane or PB exposure (t=28d), in comparison to indicated vehicle control treatments. (B) *Meg3* expression analysis in WT and CAR^{KO}/PXR^{KO} mice after 28 days of chlordane treatment (t=28d) as compared to vehicle treated samples. (C) *Cyp2b10* expression analyses across indicated mouse models after 28 days PB or chlordane treatment (t=28d). (D) human *CAR* (*hCAR*) expression analysis across indicated mouse models after 28 days of treatments (t=28d). Expression levels are indicated as mean ± SEM (n=5 biological replicates/group). Data were analyzed using GraphPad Prism 7.0. All

expression analyses are based on qPCR, primer sequences are provided in (Lempiainen et al. 2013) and Supplementary Materials and Methods. Statistical significance of treated versus untreated (vehicle) qPCR signal differences were tested using unpaired t-tests with Welch's correction for unequal variance, *p<0.05, **p<0.01, ***p<0.001, ****p<0.0001. Vehicle controls: Water (H_2O) and Corn Oil (CO).

Figure 3. Proteomic analysis of Phase I cytochrome P450 (Cyp) expression in WT and CAR^h PXR^h mice. Quantitative measurement of peptides using *in vivo* 'stable isotope labeling with amino acids in cell culture' (SILAC) technique from PB treated (A) and chlordane treated (B) liver samples, in comparison with indicated vehicle controls, in WT (filled bars) and in CAR^h/PXR^h (hatched bars) mice after 28 days of treatment (t=28d). Corresponding proteins are named on the X axis; the Y axis is expressed in fold change expression, based of vehicle expression value. Arrows indicate the metabolic enzymes concerned by the decreased signal in chlordane treated CAR^h/PXR^h samples as compared to WT samples. Protein levels are indicated as mean ± SEM (H_2O and phenobarbital n=5 biological replicates/group; CO and Chlordane n=3 biological replicates/group). Data were analyzed using GraphPad Prism 7.0. Statistical significance of treated versus untreated (vehicle) signal differences were tested using multiple unpaired t-tests on log2 transformed data. The p-values were adjusted using Holm-Sidak method, *p<0.05, **p<0.01, ***p<0.001. Vehicle controls: Water (H_2O) and Corn Oil (CO)

Figure 4. Cross-compound comparison of microarray-based xenobiotic metabolism and *Dlk1-Dio3* lncRNAs transcriptional expression profiles. *In vivo* study samples from indicated compound classes were profiled by Affymetrix microarray and specific gene expression signatures (phase I and phase II xenobiotic genes and progressive *Dlk1-Dio3* encoded Meg3 lncRNA expression) extracted and compared. Probes set expression values were summarized by gene and expressed in Log_2 fold change (Log_2FC) expression, calculated on the average of the 5 replicates (treated *versus* control). Significant difference between vehicle and treated conditions were tested with the limma package with the Benjamini-Hochberg method correction applied (Klipper-Aurbach et al. 1995; Smyth, Michaud, and Scott 2005), *p<0.05, **p<0.01, ***p<0.001, ****p<0.0001. NGC: Non-genotoxic carcinogen, NC: non-carcinogen, CPA: cyproterone acetate, DCB: 1,4-dichlorobenzene, Mpy: Methapyrilene, PB: phenobarbital, PBO: piperonyl butoxide, Wy: pirinixic acid, Pio: pioglitazone.

Figure 5. Updated model for NGC-induced pertrubation of the *Dlk1-Dio3* cluster lncRNA and xenobiotic response (modified from (Lempiainen et al. 2013))**.** Direct CAR activators or indirect compounds acting through cellular transducers (green triangle, e.g. as described in (Mutoh et al. 2013)) regulate the expression of CAR-dependent xenobiotic genes. The β-catenin pathway regulates expression of xenobiotic metabolic genes in a context dependent manner (Braeuning et al. 2009). Within WNT positive domains (e.g. perivenous hepatocytes) CAR activation is also associated with *Dlk1-Dio3* cluster ncRNAs expression. The current model acknowledges the presence of intermediate/uncharacterized co-effectors (orange hexagons) acting downstream CAR activation, and possibly linking the constitutive

xenobiotic metabolism and the progressive CAR/β-catenin dependent response. The upregulation of *Dlk1-Dio3* cluster ncRNAs might contribute to hepatocyte hypertrophy and reprogramming (Luk et al. 2011), while xenobiotic response may lead to oxidative stress through the production of reactive metabolites (Omura et al. 2014), both contributing potential key events in drug-induced tumor promotion.

Supplementary Figure legends

Supplementary Figure S1. **RT-qPCR analyses of *Dlk1-Dio3* cluster and *Cyp2b10* gene expression following 28 day compound withdrawal.** Gene expression measurement of (A) *Dlk1-Dio3* coding (*Dlk1* and *Dio3)* and non-coding RNAs (*Meg3, anti-Rtl1, Rian, Mirg*) and (B) *Cyp2b10* after treatment regimen (t=91 days in H_2O-phenobarbital study and t=28 days in CO-chlordane study) followed by 28 days of compound withdrawal (t=119 and t=56 days respectively). Expression levels are indicated as mean ± SEM (n=5 biological replicates/group). Data were analyzed using GraphPad Prism 7.0. Statistical significance of treated versus untreated (vehicle) qPCR signal differences were tested using unpaired t-tests with Welch's correction for unequal variance, *p<0.05, **p<0.01, ***p<0.001. Vehicle controls: Water (H_2O) and Corn Oil (CO).

Supplementary Figure S2. **Proteomics and gene expression profiles comparison of a panel of PB-responsive xenobiotic metabolism proteins.** Probes set expression values were summarized by (A) gene, and (B) protein expression, deducted from SILAC peptide measurement, are expressed in $\log_2$ fold change (Log_2FC) expression, calculated on the average of the 5 replicates (treated *versus* control). Vh_1016 to Vh_1020 and WT_V1 to WT_V5 correspond to vehicle treated samples, PB_2016 to PB_2020 and WT_PB1 to WT_PB5 correspond to Phenobarbital treated samples for gene expression and protein expression analyses respectively. Hierarchical clustering was performed for individual animal group and gene/protein expression.

Supplementary Figure S3. **Proteomics analysis of non-Cyp phase I protein expression in WT and CAR^h PXR^h mice.** Quantitative measurement of peptides using the 'stable isotope labeling with amino acids in cell culture' (SILAC) technique from (A) PB treated and (B) chlordane treated liver samples, in WT (filled bars) and in CAR^h PXR^h (hatched bars) mice. Corresponding proteins are named on the X axis; the Y axis is expressed in fold change expression, based of vehicle expression value. Arrows indicate the metabolic enzymes concerned by the decreased signal in chlordane treated CAR^h/PXR^h samples as compared to WT samples. Protein levels are indicated as mean ± SEM (H_2O and phenobarbital n=5 biological replicates/group; CO and Chlordane n=3 biological replicates/group).Data were analyzed using GraphPad Prism 7.0. Statistical significance of treated versus untreated (vehicle) signal differences were tested using multiple unpaired t-tests on log2 transformed data. The p-values were adjusted using Holm-Sidak method, *p<0.05, **p<0.01. Vehicle controls: Water (H_2O) and Corn Oil (CO).

Supplementary Figure S4. Proteomics analysis of phase II protein expression in WT and CAR^h PXR^h mice. Quantitative measurement of peptides using the *in vivo* 'stable isotope labeling with amino acids in cell culture' (SILAC) technique from (A) PB treated and (B) chlordane treated liver samples, in WT (filled bars) and in CAR^h PXR^h (hatched bars) mice. Corresponding proteins are named on the X axis; the Y axis is expressed in fold change expression, based of vehicle expression value. Protein levels are indicated as mean ± SEM (H_2O and phenobarbital n=5 biological replicates/group; CO and Chlordane n=3 biological replicates/group). Data were analyzed using GraphPad Prism 7.0. Statistical significance of treated versus untreated (vehicle) signal differences were tested using multiple unpaired t-tests on

log2 transformed data. The p-values were adjusted using Holm-Sidak method, *p<0.05, **p<0.01, ***p<0.001, ****p<0.0001. Vehicle controls: Water (H_2O) and Corn Oil (CO).

Supplementary Figure S5. Role of *Dlk1-Dio3* non-coding RNAs in liver cancer and their potential relevance as non-genotoxic carcinogenesis biomarkers. (A) The potential relevance of mechanisms of drug-induced tumors in humans is frequently investigated by integrating tissue histopathology and biochemical and molecular indicators of neoplastic risk. Mechanistic studies that integrate phenotypically-anchored molecular and biochemical biomarkers have the potential to provide mechanistic insights to help evaluate early on the risk for drug induced carcinogenesis, as well as support the interpretation of drug-induced tumors and in some cases provide valuable perspectives on potential relevance in humans (Moggs et al. 2016). (B) Phenobarbital case study exemplifying the identification of *Dlk1-Dio3* imprinted gene cluster noncoding RNAs as novel candidate biomarkers for phenobarbital-induced liver tumor promotion (Lempiainen et al. 2013). Pathway dependence (CAR and β-catenin) and phenotypic anchoring (e.g. tissue localization, phenotype), represent important steps of the candidate biomarker characterization. (C) Deregulation of the *Dlk1-Dio3* cluster was observed in numerous developmental disorders and neoplasia, including hepatocellular carcinoma in humans and in mouse models. *Dlk1-Dio3* associated non-coding RNA (including *Meg3*) genetically and biochemically interact and regulate a number of important cellular processes whose deregulation may be critical for tumor promotion and progression. snoRNA, small nucleolus RNA.

Supplementary Table legends

Supplementary Table S1. **List of model compounds and associated study designs.** The compound class, known mechanism of action, link to CAR dependency and a summary of the *in vivo* experimental conditions are shown. GC: genotoxic carcinogenesis, NGC: non genotoxic carcinogenesis, CMC: carboxy-methyl cellulose, po: oral intake, ip: intraperitoneal injection.

Supplementary Table S2. **List of selected xenobiotic metabolism genes, representing candidate CAR-activation dependent signature.** The original study design contributing to the identification of the selected genes is indicated. po: oral intake, ip: intraperitoneal injection.

Supplementary Table S3. Microarray data of selected xenobiotic metabolism genes and *Dlk1-Dio3* cluster ncRNAs. The table indicates RMA-normalized and summarized by gene Log_2FC between treated and vehicle samples and adjusted p-values using the Benjamini-Hochberg method. The study ID indicates the key study and compound information. The drug, genetic background and time of treatment are indicated.

Tables

Table 1. Phenobarbital and chlordane lead to comparable liver phenotype *in vivo*. Toxicological and pathological data after 28 days (t=28) chlordane and 28 (t=28) or 91 (t=91) days PB treatment (Main) are shown. Recovery (Rec) was run for an additional 28 days for the chlordane and phenobarbital studies (t=56 and t=119 respectively). Body weight and plasma concentrations are indicated as mean value of indicated (n) individuals per group ± standard deviation. *In vivo* data referring to the phenobarbital study are adapted from (Luisier et al. 2014). Centrilobular hypertrophy severity grades were on a 0-4 scale, expressed as median (n=5).

	phenobarbital									chlordane					
	wild - type			CAR^{h} – PXR^{h}			CAR^{KO} - PXR^{KO}			wild - type		CAR^{h} – PXR^{h}		CAR^{KO} - PXR^{KO}	
	Main t=28	Main t=91	Rec t=119	Main t=28	Main t=91	Rec T=119	Main t=28	Main t=91	Rec t=119	Main t=28	Rec t=56	Main t=28	Rec t=56	Main t=28	Rec t=56
Body weight	27.6 ± 2.2 n=15	33.9 ± 2.8 n=10	33.1 ± 1.7 n=5	26.5 ± 1.3 n=15	31.0 ± 2.5 n=10	31.3 ± 2.4 n=5	27.8 ± 2.1 n=15	31.5 ± 4.7 n=10	30.6 ± 4.4 n=5	24.6 ± 1.2 n=10	26.2 ± 2.4 n=5	25.5 ± 1.8 n=10	23.77 ± 1.1 n=5	25.3 ± 1.3 n=10	25.6 ± 0.8 n=5
Plasma concentration (µg/mL) n=5	19.7 ± 3.6	11.1 ± 3.2	0.0 ± 0.0	32.3 ± 5.2	17.0 ± 7.2	0.0 ± 0.0	82.7 ± 8.9	52.6 ± 6.3	0.0 ± 0.0	7.7 ± 3.5	1.0 ± 0.4	4.8 ± 1.2	2.3 ± 2.0	5.2 ± 2.0	2.1 ± 1.3
Centrilobular hypertrophy (score 0:4) Median	2	3	2	3	3	1	0	1	0	3	2	3	2	0	0

Luisier, R., H. Lempiainen, N. Scherbichler, A. Braeuning, M. Geissler, V. Dubost, A. Muller, N. Scheer, S. D. Chibout, H. Hara, F. Picard, D. Theil, P. Couttet, A. Vitobello, O. Grenet, B. Grasl-Kraupp, H. Ellinger-Ziegelbauer, J. P. Thomson, R. R. Meehan, C. R. Elcombe, C. J. Henderson, C. R. Wolf, M. Schwarz, P. Moulin, R. Terranova, and J. G. Moggs. 2014. 'Phenobarbital induces cell cycle transcriptional responses in mouse liver humanized for constitutive androstane and pregnane x receptors', *Toxicol Sci*, 139: 501-11.

Figure 1. Pouché Vitobello *et al.*

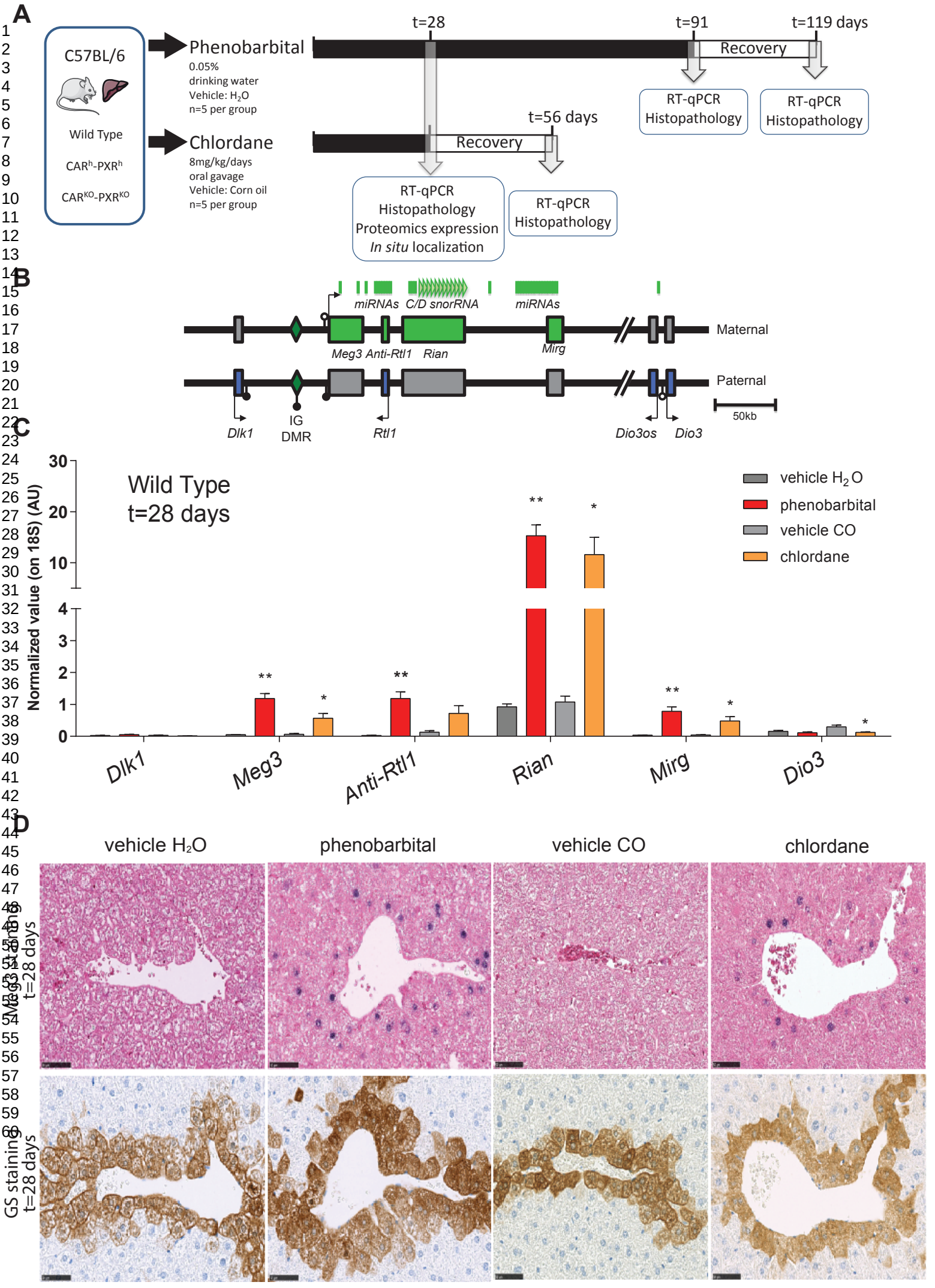

Figure 2. Pouché, Vitobello *et al.*

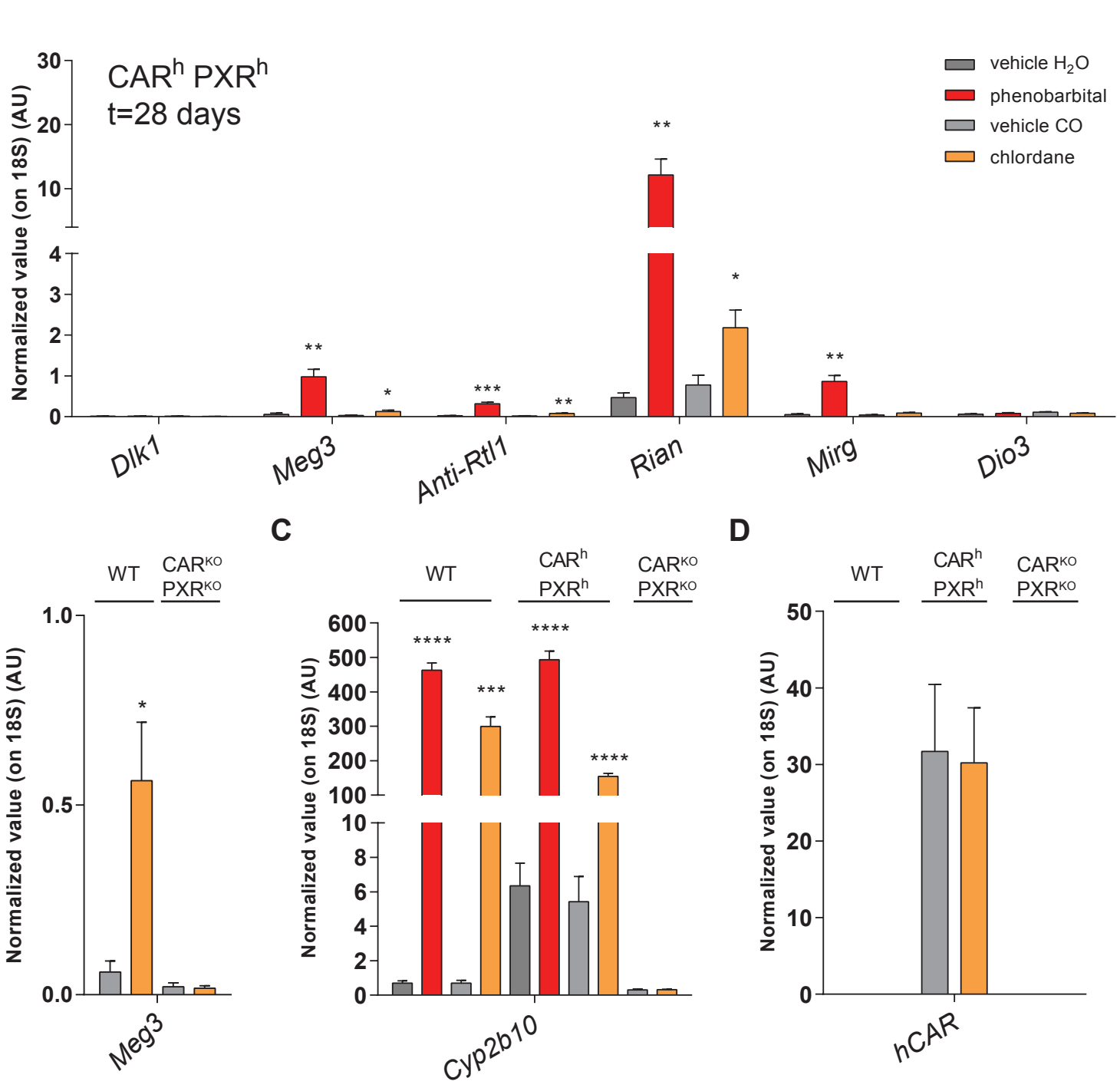

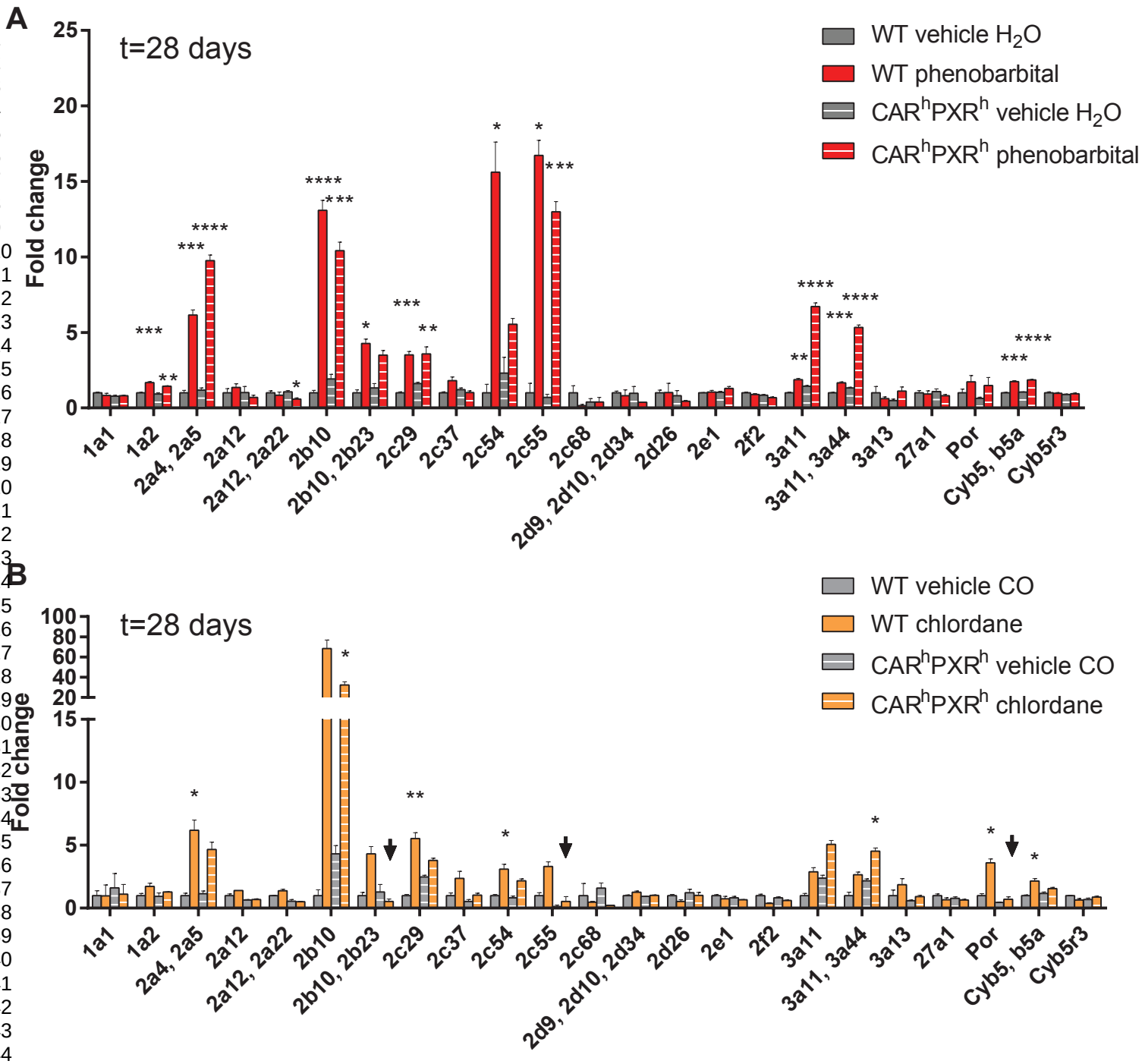
A
t=28 days
Fold change
WT vehicle H2O
WT phenobarbital
CARhPXRh vehicle H2O
CARhPXRh phenobarbital
1a1
1a2
2a4, 2a5
2a12
2a12, 2a22
2b10
2b10, 2b23
2c29
2c37
2c54
2c55
2c68
2d9, 2d10, 2d34
2d26
2e1
2f2
3a11
3a11, 3a44
3a13
27a1
Por
Cyb5, b5a
Cyb5r3
B
t=28 days
Fold change
WT vehicle CO
WT chlordane
CARhPXRh vehicle CO
CARhPXRh chlordane

Figure 4. Rouché, Vitobello *et al.*

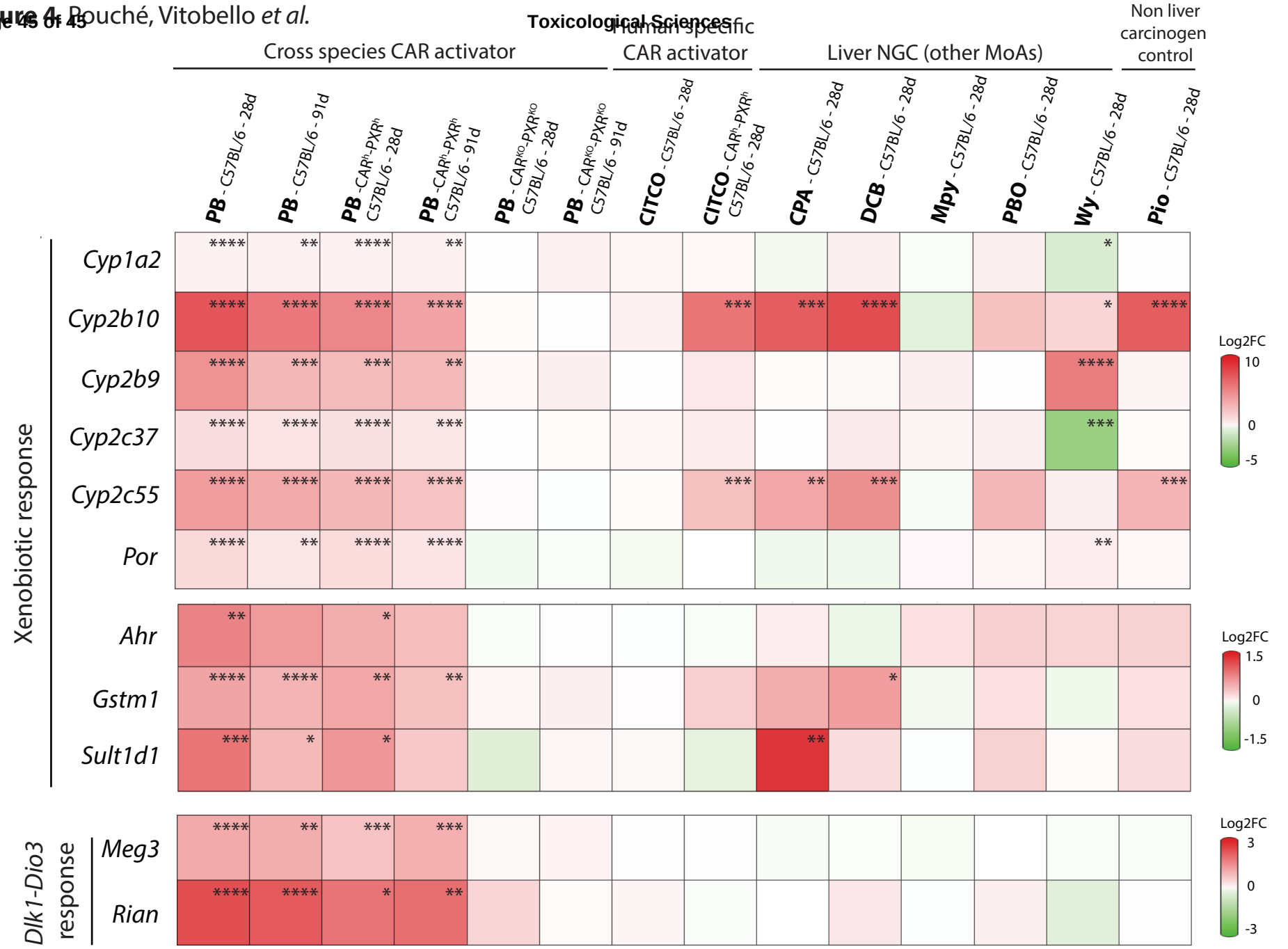

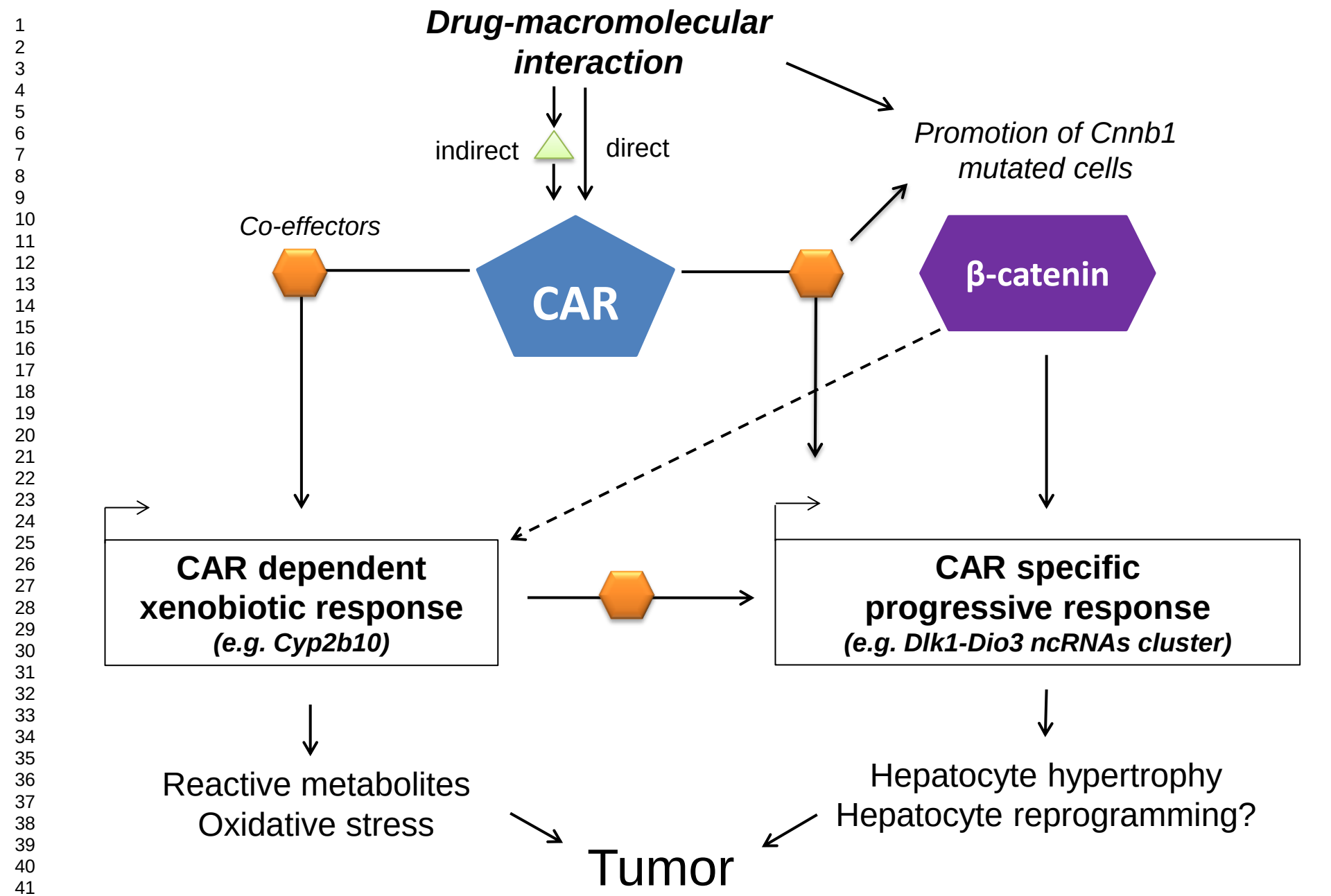
Drug-macromolecular interaction
indirect
direct
Promotion of Cnnb1 mutated cells
Co-effectors
CAR
β-catenin
CAR dependent xenobiotic response
(e.g. Cyp2b10)
CAR specific progressive response
(e.g. Dlk1-Dio3 ncRNAs cluster)
Reactive metabolites
Oxidative stress
Hepatocyte hypertrophy
Hepatocyte reprogramming?
Tumor